Fuel 116 (2014) 242–254

Contents lists available at ScienceDirect

Fuel

journal homepage: www.elsevier.com/locate/fuel

Speed of sound in pure fatty acid methyl esters and biodiesel fuels

André F.G. Lopes [a], Maria del Carmen Talavera-Prieto [b], Abel G.M. Ferreira [b,*], Jaime B. Santos [a], Mário J. Santos [a], António T.G. Portugal [b]

[a] Department of Electrical and Computers Engineering, University of Coimbra, Polo II, Rua Silvio Lima, 3030-970 Coimbra, Portugal
[b] Department of Chemical Engineering, University of Coimbra, Polo II, Rua Silvio Lima, 3030-970 Coimbra, Portugal

HIGHLIGHTS

- New data on sound speed is reported for fatty acid methyl esters.
- New data on speed of sound is reported for biodiesel fuels.
- Molar compressibility was calculated for fatty acid methyl esters and biodiesel.
- Predictive models for speed of sound and molar compressibility are proposed.

ARTICLE INFO

Article history:
Received 7 June 2013
Received in revised form 12 July 2013
Accepted 16 July 2013
Available online 31 July 2013

Keywords:
Biodiesel
Speed of sound
Compressibility
Correlation

ABSTRACT

The property changes associated with the differences in chemical composition of biodiesel may change the fuel injection timing which in turn cause different exhaust emissions and performance of engines. The property that has an important effect on the fuel injection timing is the speed of sound (related with isentropic bulk modulus). Despite the speed of sound of pure fatty acid (methyl and ethyl) esters being reasonably known in a wide range of temperature the experimental data for biodiesel are very scarce in the literature. In this work the speed of sound of six fatty acid methyl esters (FAME = laurate (MeC12:0), myristate (MeC14:0), palmitate (MeC16:0), stearate (MeC18:0), oleate (MeC18:1), linoleate (MeC18:2)) and six biodiesel fuel samples were measured using a non-intrusive ultrasonic methodology. The measurements for FAMEs were made at atmospheric pressure from a minimum of 288.15 K to a maximum of 353.15 K, and in the temperature range 298.15–353.15 K for biodiesel samples. The uncertainty of the measurements was estimated as less than ±1 m s^{-1}. The speed of sound data combined with available density data from literature was used to calculate the isentropic compressibility and the molecular compressibility for the FAMEs and for the biodiesel samples. The results for molecular compressibility evidenced that this property is almost independent of the temperature in the temperature range of calculations both for FAMES and biodiesel. Linear relationships were established between the molar compressibility and the molecular weight for FAMES and biodiesel. The before mentioned behavior of molar compressibility face to temperature and molecular weight make it possible to develop prediction methods for the calculation of the speed of sound.

1. Introduction

The conventional fossil fuels (petrofuels) are non-renewable, increasingly scarce, with growing emissions of combustion resulting pollutants, and with increasing costs of production. On the other hand, fuel reserves are concentrated in certain planet regions and most of them are reaching the production peak. All these circumstances make biomass sources more attractive in particular the biodiesel. Unlike petrodiesel, biodiesel is a renewable fuel offering important benefits including reduction of green-house emissions, biodegradability, and non-toxicity. Biodiesel shows total miscibility with petrodiesel and compatibility with modern engines [1,2]. Nowadays, biodiesel production has important economic and social impacts at the regional development level especially to developing countries [3]. Technically, biodiesel is a fuel formed by long chain of fatty acid esters produced from a large variety of feedstocks including vegetable oils and animal fats, with designation of B100, meeting the property and quality requirements of the American Society Testing (ASTM) D6751 standard. Biodiesel can be produced through transesterification chemical reaction along which the raw material reacts with alcohol (usually methanol or ethanol) in the presence of a catalyst that can be metal alkoxide [4], ionic liquids [5], or others [6]. The resulting products

* Corresponding author. Tel.: +351 239 798 729; fax: +351 239 798 703.
E-mail address: abel@eq.uc.pt (A.G.M. Ferreira).

0016-2361/$ - see front matter © 2013 Elsevier Ltd. All rights reserved.
http://dx.doi.org/10.1016/j.fuel.2013.07.044

are the fatty acid (methyl or ethyl) esters (FAE or biodiesel) and glycerol.

Glycerol, which is a high value byproduct of the transesterification reaction forms one phase and (FAE) form another phase, which settles above the glycerol in the reactor. The biodiesel fuel must meet specifications contained in biodiesel standards, such as the (ASTM) D6751 and the EN14214 in Europe. Some of these specifications are related to the fuel quality such as completeness of transesterification reaction, storage conditions and other important properties as viscosity, density, oxidative stability, cetane number, and cold flow properties, depending all on the fatty acid composition of biodiesel. The injection process is of great importance for engine efficiency. In this process an appropriate quantity of fuel is feed to the engine cylinder forming a spray of tiny fuel droplets to optimize the combustion and reduce the fuel consumption and emissions. All injection process is strongly influenced by the thermophysical fuel properties. The properties of major influence in the injection time are the surface tension [7], the viscosity, and the isentropic bulk modulus [8], which is determined by the sound speed. Therefore, for the accurate design and maintenance of injection systems, the accurate knowledge of the sound speed of the fuel plays an important role. Biodiesel sound speed information is very scarce in the literature, although several authors have measured this property for pure methyl and ethyl FAEs. Some previous literature reports on speed of sound of pure FAMEs and biodiesel are summarized in Table 1, calculated for different temperature and pressure ranges, techniques and uncertainties of the measurements.

This work aims to evaluate the sound speed of pure liquid FAMEs most frequently found in biodiesel, and also of the biodiesel fuels. This property has been measured for MeC12:0, MeC14:0, MeC16:0, MeC18:0, MeC18:1, MeC18:2 considering wide ranges

Table 1
Previous sources of data for the speed of sound of the FAME compounds studied herein and biodiesel.

Authors	Year	N_p	T (K)	P (MPa)	(u) and (σ_u (m s^{-1})[a]	Method[b]	Purity (wt%)
Mehyl laurate (MeC12:0)							
Gouw and Vlugtert [9]	1964	2	293, 313	0.1	(1278, 1351) (0.08%)	Interf	>99.7
Tat and Gerpen [10][c]	2003	–	293–373	0.1–32.5	(1086–1502) (0.1–0.7%)	PE	[d]
Tat and Gerpen, NREL[11]	2003	30	293–373	0.1–34.5	(1080–1498) (0.1–0.7%)	PE	[d]
Freitas et. al. [12]	2013	12	288–343	0.1	(1171–1370) (0.01)	PE	97
Methyl myristate (MeC14:0)							
Gouw and Vlugtert [9]	1964	2	293, 313	0.1	(1299, 1372) (0.08%)	Interf	>99.7
Freitas et. al. [12]	2013	10	298–343	0.1	(1194–1353) (0.01)	PE	98
Daridon et. al. [13]	2013	8	303–373	0.1	(1098–1335) (<0.1%)	PE	99
Ndiaye et al. [14]	2013	53	303–393	0.1–80	(1036–1614) (0.2%)	PE	99
Methyl palmitate (MeC16:0)							
Gouw and Vlugtert [9]	1964	1	313	0.1	(1318) (0.08%)	Interf	>99.7
Tat and Gerpen [10][c]	2003	–	293–373	0.1–32.5	(1123–1537) (0.1–0.7%)	PE	>99
Tat and Gerpen, NREL[11]	2003	24	313–373	0.1–34.5	(1019–1463) (0.1–0.7%)	PE	[e]
Ott et al. [15]	2008	7	308–338	0.1	(1233–1338) (0.1%)	PE	>99.0
Daridon et. al. [13]	2013	7	313–373	0.1	(1171–1370) (<0.1%)	PE	99
Ndiaye et al. [14]	2013	35	303–393	0.1–50	(1057–1507) (0.2%)	PE	99
Freitas et al. [16]	2013	8	308–343	0.1	(1216–1337) (0.02)	DSA5000	99
Methyl Stearate (MeC18:0)							
Gouw and Vlugtert [9]	1964	1	313	0.1	(1333) (0.08%)	Interf	>99.7
Tat and Gerpen [10][c]	2003	–	293–373	0.1–32.5	(1141–1541) (0.1–0.7%)	PE	>99
Ott et al. [15]	2008	5	318–338	0.1	(1248–1317) (0.1%)	PE	>99.0
Freitas et al. [16]	2013	7	313–343	0.1	(1231–1333) (0.02)	DSA5000	99
Methyl oleate (MeC18:1)							
Gouw and Vlugtert [9]	1964	2	293, 313	0.1	(1338–1408) (0.08%)	Interf	>99.7
Ott et al. [15]	2008	7	278–338	0.1	(1250–1462) (0.1%)	PE	>99.0
Freitas et. al. [12]	2013	12	288–343	0.1	(1238–1427) (0.01)	PE	99
Daridon et. al. [13]	2013	10	283–373		(1139–1446) (<0.1%)	PE	99
Methyl linoleate (MeC18:2)							
Gouw and Vlugtert [9]	1964	2	293, 313	0.1	(1348–1419) (0.08%)	Interf	>99.7
Tat and Gerpen [10][c]	2003	–	293–373	0.1–32.5	(1156–1554) (0.1–0.7%)	PE	[f]
Tat and Gerpen, NREL[11]	2003	30	293–373	0.1–34.5	(1151–1550) (0.1–0.7%)	PE	[f]
Ott et al. [15]	2008	7	278–338	0.1	(1260–1472) (0.1%)	PE	>99.0
Daridon et. al. [13]	2013	10	283–373	0.1	(1149–1456) (<0.1%)	PE	99
Freitas et al. [16]	2013	11	288–343	0.1	(1246–1418) (0.02)	DSA5000	99
Biodiesel							
Tat and Gerpen [10,11]	2003	384	293–373	0.1–34.5	(1053–1551) (0.1–0.7%)	PE	–
Huber et al. [17]	2009	14	278–333	0.08	(1255–1467) (0.03–1.00)	PE	[g]
Payri et al. [18][c]	2011	–	298–343	15–180	(1213–1848) (≈0.3%)	TOF	[h]
Nicolic et al. [19][c]	2012	17	293	0.1–160	(1404–1893) (0.05)	PE	[i]
Freitas et al. [12]	2013	120	288–343	0.1	(1230–1432) (0.01)	DSA5000	[j]

[a] The uncertainty in speed of sound (σ_u) is given in m s^{-1} or percentage.
[b] Interf: interferometer; PE: pulse-echo; TOF: time of flight.
[c] Data is given in expression(s) form(s).
[d] Sample: MeC12:0 (99.2), MeC18:1 (0.6), and MeC18:2 (0.2).
[e] Sample: MeC12:0 (0.2), MeC14:0 (4.6), MeC16:0 (88.2); MeC17:0 (0.4), and MeC18:0 (6.3).
[f] Sample: MeC16:0 (1.4), MeC18:0 (0.7), MeC18:1 (5.2), MeC18:2 (86.5), and MeC18:3 (6.2).
[g] Two commercial samples from rapeseed oil were used.
[h] Rape methyl ester used in Spain.
[i] Rape methyl ester used in Serbia.
[j] Samples synthesized at laboratory: soybean (S), rapeseed (R), palm (P), soybean + rapeseed (SR), palm + rapeseed (PR), soybean + palm (SP), soybean + rapeseed + palm (SRP), sunflower (SF); from Portuguese biodiesel producers: soybean + rapeseed (GP) and SoyA.

Table 2
Sample material purities of the calibration standards and FAMEs.

Material	Supplier	Cas No.	Sample purity (wt%)	Structure/properties
Water			Mili-Q	
Toluene	Acros Organics	142–82–5	99.9	
2-Butanediol	Carlo Erba	64–17–5	99.9	
Methyl laurate	Sigma Aldrich	111–82–0	>97	
Methyl myristate	Sigma Aldrich	124–10–7	>98	
Methyl palmitate	Sigma Aldrich	112–39–0	>97	
Methyl stearate	Sigma Aldrich	112–61–8	>96	
Methyl oleate	Sigma Aldrich	112–62–9	>99 GC	
Methyl linoleate	Acros Organics	112–63–0	>99 GC	
Cotton seed oil	Acros Organics	17711	Fatty acid composition: MeC14:0 and lower: ca 1.5%; MeC16:0 ca 25%; MeC18:0 ca 3%; MeC18:1, 16 to 24%; MeC18:2, 50 to 55%; MeC18:3 and higher < 1.5%	AV ⩽ 0.5 mg KOH g^{-1} SV = 185–198 mg KOH g^{-1}; IV = 95–115 g I/100 g, UM < 1.5%; n = 1.4720–1.4730 (20 °C, 589 nm)

AV = acid value; SV = saponification value; IV = iodine value; UM = unsaponifiable matter; n = refractive index.

of temperatures. Additionally, five synthetic biodiesel samples composed by different FAMEs were prepared, and also a cotton seed biodiesel sample was produced by transesterification of the cotton seed oil, then measuring the respective speed of sound. The measurements are reported at atmospheric pressure and temperatures ranging from 298.15 to 353.15 K. The speed of sound was combined with density to calculate the isentropic and molecular compressibilities for the FAMEs and biodiesel samples studied in this work. We have also used additional information of speed of sound for FAMEs and biodiesel samples from literature to extend and complete the knowledge of the molecular compressibility. From all the collected information, predictive models of molecular compressibility and speed of sound for FAMEs and biodiesel were formulated.

Table 3
Biodiesel composition (wt%) of biodiesel of this study.

Biodiesel FAME	SCS[a]	SBT[b]	SPF[c]	SYG1[d]	SYG2[d]	PCS[e]
MeC14:0	0.93	0.50	0.94	0.00	2.83	0.01
MeC16:0	24.98	17.00	25.56	11.90	28.57	26.76
MeC18:0	2.66	9.41	7.83	14.43	13.07	2.81
MeC18:1	18.48	31.24	36.34	72.46	46.60	17.89
MeC18:2	52.94	41.85	29.32	1.21	8.92	51.60

[a] SCS: synthetic cotton seed oil.
[b] SBT: synthetic beef tallow.
[c] SPF: synthetic biodiesel poultry fat.
[d] SYG1 and SYG2: synthetic samples from yellow grease.
[e] PSB: Produced cottonseed biodiesel.

2. Experimental

2.1. Calibration liquids and fuels

Water (mili-Q), toluene obtained from ACROS (Cas No: 142–82-5) with a mass fraction purity of 99.9 wt%, and 2-butanediol from Carlo Erba (Cas No. 64–17-5) with a stated mass fraction of 99.9 wt% have been used as speed of sound calibrant liquids in the cell. The liquids were previously degassed ultrasonically.

The methyl esters (MeC12:0, purity ⩾ 97%, wt%), (MeC14:0, purity ⩾ 98%), (MeC16:0, purity ⩾ 97%), (MeC18:0, purity ⩾ 96%), (MeC18:1, purity ⩾ 99%, GC grade), were purchased from Sigma Aldrich and (MeC18:2, purity ⩾ 99%, GC) from Acros Organics. All the FAMEs were used without further purification. Five synthetic biodiesel samples were prepared from known masses of FAMEs (MeC14:0, MeC16:0, MeC18:0 MeC18:1, and MeC18:2). Also, one biodiesel sample was produced by trasesterification of cottonseed oil, which was supplied by Acros Organic. The detailed specifications of all materials are summarized in Table 2.

2.2. Synthetic samples and cottonseed biodiesel preparation

The composition choice for the synthetic samples was based on the availability of their experimental cetane number once we intend to study this important parameter in a future work. The idea was to choose samples that could allow covering a wide range of cetane numbers, with specifications of regulatory standards. Methyl esters were mixed in appropriate mass proportions to simulate the target biodiesel samples. The biodiesel samples were prepared as follows: the synthetic cottonseed (SCS) biodiesel was based on the compositions reported by Wadumesthrige et al. [20]; the synthetic beef tallow (SBT) was from the composition given by Ramirez-Verduzco et al. [21]; synthetic biodiesel poultry fat (SPF) was obtained from composition reported by Wadumesthrige et al. [20]; two synthetic samples from yellow grease (SYGI and SYGII), obtained from cooking oil used in “fast food” were prepared from the composition reported by Kinast [22] and Canacki and Gerpen [23], respectively. The composition of synthetic biodiesel samples are presented in Table 3. The transesterification of cottonseed oil was carried out in a 50 ml three-necked double wall jacketed reactor. The reactor was equipped with a reflux condenser, to avoid methanol losses, a magnetic stirrer, a digital thermometer (ERTCO-EUTECHNICS Model 4400 Digital thermometer) and one stopper to feed the raw materials. The reactor was initially charged with a known amount of oil. A solution of known amount of catalyst sodium methoxide was prepared in the required amount of methanol and was added to the oil sample. After proper closing of the flask the temperature in the reactor was maintained constant by circulating water from a thermostatic bath (Digiterm 100 JP SELECTA). The system was also kept airtight to prevent the loss of alcohol. The reaction mix was held at a temperature just above the boiling point of the alcohol i.e. around 65 °C to speed up the reaction. The reaction time was 2 h. Excess alcohol was normally used to ensure total conversion of the oil to its esters. After the confirmation of completion of methyl ester formation, the heating was stopped and the products were cooled and transferred to a separating funnel. The ester layer containing mainly methyl esters and methanol and the glycerol layer containing mainly glycerol and methanol were separated. The methyl esters were washed and dried under vacuum to remove traces of moisture.

2.3. Analyticalmethods

The FAMEs of biodiesel produced from cottonseed oil supplied by Acros Organic, was analyzed by gas chromatography in a TRE METRICS 9001 gas chromatograph equipped with a 30 m fused silica capillary column DB-225 (J & W Scientific), Agilent with a length of 30 m, with 0.15 μm film, and an internal diameter of 0.25 mm. A sample (1 μl) was injected at temperature of 280 °C and without split. Helium was used as the carrier gas at a flow rate of 1 ml min^{-1} and also used as auxiliary gas for the FID. The following temperature ramp was used: initial temperature of 70 °C during 1 min, followed by an increase of 10 °C min^{-1} up to 180 °C and then 3 °C min^{-1} up to 220 °C, which was maintained for 15 min. The components in the product were quantified by using heptadecanoate methyl ester as an internal standard. Calibration was done using different concentrations of each methyl esters in *n*-heptane with addition of internal standard. The composition of the cotton seed biodiesel (PCS) is presented in Table 3.

2.4. Sound speed measurement

The measurement of the ultrasound velocity can provide useful information about the physicochemical behavior of liquids and liquid mixtures. Several relations and semi-empirical approaches are available in literature for the calculation of the ultrasound velocity in liquid and liquid mixtures.

In order to measure the ultrasound propagation velocity in the esters and biodiesel fuels a cell was used. A schematic of that cell is shown in Fig. 1a inserted in the measurement system and its construction details can be observed in Fig. 1b. The cylindrical cell is composed by a stainless steel hollow having diameter and length of 12 mm and 15.5 mm, respectively to accommodate the testing liquids. Two 5 MHz ultrasonic transducer are mounted in cavities drilled on the cell plane surfaces, one acting as a transmitter and the other as a receiver. To minimize reflections, the transducers are in contact with the stainless steel walls of the cavities, and silicone oil is used to enhance the wave transmission.

A wide band pulse generator is used to excite the transmitter transducer. The acoustical wave propagates through the testing liquid and is collected by the receiver. Then, the signal is amplified and displayed in the oscilloscope, and transferred to the computer for processing (see Fig. 1a). An A-scan representation of a signal corresponding to the propagation over the media between the transmitter and the receiver is shown in Fig. 2. The time of flight $\Delta\tau$ in the testing sample is obtained from the difference between the emitter-receiver propagation time and the propagation time in the steel walls (see Fig. 2). The cell was calibrated by measuring $\Delta\tau$ in water, toluene and 2-butanediol at atmospheric pressure, over the full range of temperatures $T = (298.15–343.15)$ K and $u = (1117–1602)$ m s^{-1} using a total of 22 (T, u) data points for

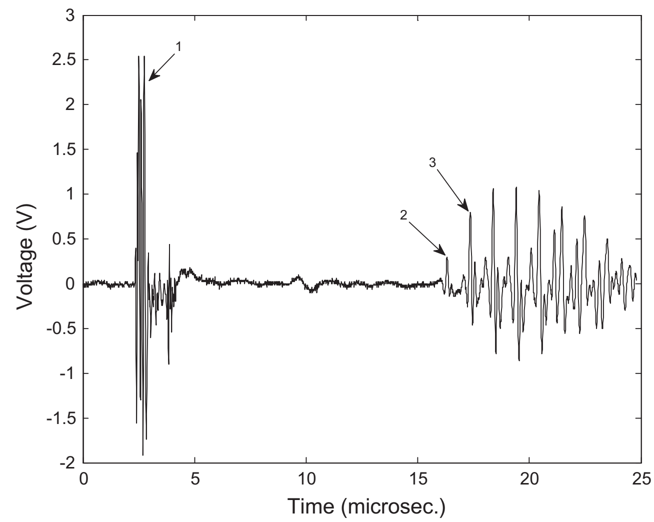

Fig. 2. S A-scan signal: (1) Emission signal; (2) receiving signal; (3) steel wall reflected signal.

these liquids (water [24], toluene [25], and 2-butanediol [26]). The literature $u(T)$ data were fitted using the following equation:

$$\frac{1}{u} = (c_1 + c_2T) + (c_3 + c_4T)\Delta\tau \quad (1)$$

where $c_1 = (-1.84069 \times 10^{-4} \pm 3.1489 \times 10^{-5})$ m^{-1} s, $c_2 = (3.45446 \times 10^{-7} \pm 9.8981 \times 10^{-8})$ m^{-1} s K^{-1}, $c_3 = (64.0477 \pm 2.0235)$ m^{-1}, and $c_4 = (-3.17784 \times 10^{-2} \pm 6.3000 \times 10^{-3})$ m^{-1} K^{-1}. The obtained correlation coefficient and standard deviation were $R = 1.000$ and $\sigma = \pm 6.30 \times 10^{-7}$ m^{-1} s, respectively. In terms of speed of sound the standard deviation and absolute average deviation AAD% are defined as:

$$\sigma = \left[\sum_{i=1}^{N_p}(u_{cal} - u_{\exp})_i^2/N_p\right]^{1/2} \quad (2)$$

$$AAD\% = (100/N_p)\sum_{i=1}^{N_p}|u_{\text{cal}}/u_{\exp} - 1|_i \quad (3)$$

where the subscripts "exp" and "cal" are used for experimental and calculated values (*vd*. Eq. (1)), respectively, and N_p is the number of

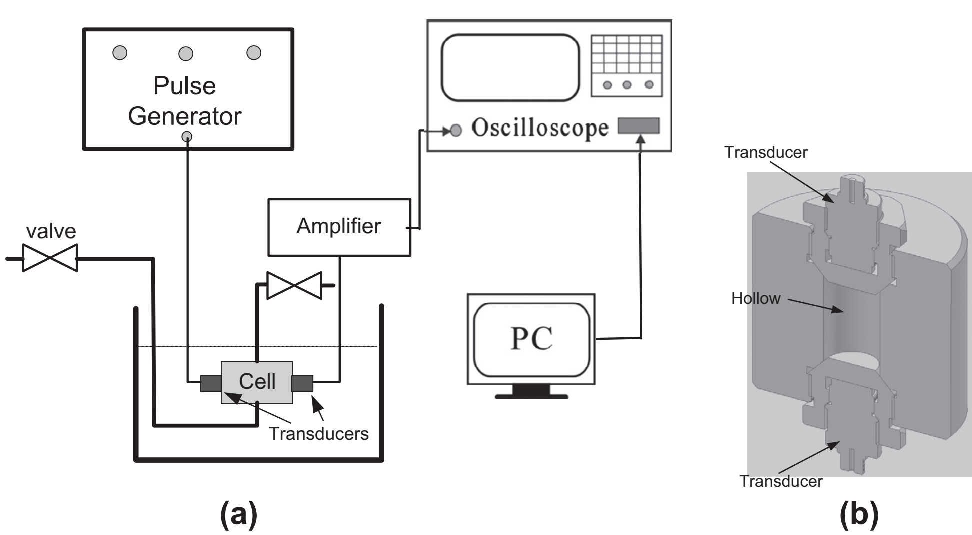

Fig. 1. Scheme of speed of sound measurement system. (a) Ultrasound cell and peripheral equipment. (b) Ultrasound cell details.

data points. The values $\sigma = \pm 1.2\ \mathrm{m\,s^{-1}}$ and AAD% = 0.07% were obtained.

3. Results and discussion

3.1. Sound speed

The speed of sound measured at extended ranges of temperature for several FAMEs and biodiesel here studied are given in Table 4. The following polynomial expression, the equation:

$$u = \sum_{i=0}^{2} u_i T^i \quad (4)$$

was fitted to the experimental (T,u) and the obtained coefficients u_i are shown in Table 5. The coefficient of correlation, the low standard deviation and AAD% values reveal the good quality of measured data (T,u). The second degree polynomial accounts for the slight curvature sometimes observed in (T,u) data. This behavior is particularly seen for water used here as calibration fluid. The experimental speed of sound for the studied samples, calculated from the A-Scan data (see Fig. 2) versus temperature are illustrated in Fig. 3. The melting points of the FAMEs given by Knothe and Dunn [27] are also shown. It can be seen that the speed of sound decreases with the increase of temperature as expected, with almost the same slopes, and the saturated and unsaturated MeC18 show similar values of speed of sound, where the differences are less than $10\ \mathrm{m\,s^{-1}}$. This is important because most of biodiesel systems are formed mainly by MeC18 FAMEs of several degrees of saturation. The speed values for biodiesel at a given temperature are similar to those of MeC18 FAMEs as illustrated in Table 4. The experimental speed of sound values were compared with the ones from literature (see Figs. 4–6). It can be affirmed that the sound speed values obtained in this work are in agreement with the ones provided by the literature, presenting relative deviations less than 0.3%, which corresponds *ca.* $4\ \mathrm{m\,s^{-1}}$, except for the results by Tat and van Gerpen [11]. The experimental speed of sound in synthetic samples and in the produced cottonseed biodiesel are shown in Fig. 7. It can be observed that they fall in a narrow range of *ca.*11 $\mathrm{m\,s^{-1}}$, and this range is almost independent of the temperature. The experimental values of Freitas et al. [12] for soy and palm methylic biodiesel were included for purpose of comparison. All the other biodiesel samples studied by Freitas et al. have (T,u) values into the before mentioned speed of sound range.

3.2. Molar compressibility

An important parameter in the study of liquid state is the molar compressibility also called Wadás constant [28] defined by

$$k_m = \frac{M}{\rho} k_S^{-1/7} \quad (5)$$

where M is the molar mass, k_S the isentropic compressibility, and ρ the density. The isentropic compressibility k_S is calculated from the Laplace equation:

$$k_S = \left[\frac{1}{\rho}\left(\frac{\partial \rho}{\partial p}\right)_S\right] = \frac{1}{\rho u^2} \quad (6)$$

where S is the entropy, and p the pressure.

The molar compressibility is assumed to be independent of the temperature in liquids and it is obtained from integration of the differential relationship [29],

$$\left(\frac{\partial \ln k_s}{\partial T}\right)_P = -7\alpha_p \quad (7)$$

where $\alpha_P = -(1/\rho)(\partial\rho/\partial T)_P$ is the isobaric expansibility. For the saturated FAMEs MeC10:0, MeC14:0, and MeC16:0, Daridon et al. [13] found an almost constant temperature dependence of k_m and they developed a group contribution method to predict the molecular compressibility and speed of sound for methyl and ethyl esters with an uncertainty of *ca.* 0.1%. In this work, the experimental density data of Pratas et al. [30] were used to calculate the isentropic

Table 4
Experimental speed of sound (u) for FAME, synthetic and produced biodiesels at atmospheric pressure.

T/K	u / (m·s^{-1})	T/K	u / (m·s^{-1})	T/K	u / (m·s^{-1})	T/K	u / (m·s^{-1})	T/K	u / (m·s^{-1})	T/K	u / (m·s^{-1})
MeC12:0		MeC14:0		MeC16:0		MeC18:0		MeC18:1		MeC18:2	
										288.41	1434.5
										293.33	1414.5
298.25	1332.3	298.15	1350.9					298.28	1389.9	298.15	1398.3
303.17	1313.5	303.15	1331.5					303.79	1365.3	303.20	1378.5
308.26	1293.5	308.17	1312.8					308.15	1353.3	308.20	1360.3
313.15	1277.8	313.15	1296.6	313.42	1317.0			313.28	1336.0	313.15	1343.7
318.15	1258.2	318.15	1276.4	318.15	1297.0			318.15	1318.2	318.15	1327.6
323.17	1243.6	323.15	1255.3	323.17	1282.1	323.15	1297.3	323.15	1301.0	323.15	1308.3
328.17	1224.5	328.15	1243.2	328.15	1263.4	328.15	1281.7	328.15	1282.6	328.34	1288.8
333.15	1207.6	333.15	1228.2	333.15	1247.1	333.15	1263.1	333.15	1266.5	333.15	1272.5
338.15	1187.5	338.15	1212.1	338.15	1231.2	338.15	1248.4	338.15	1249.2	338.15	1255.9
343.15	1171.2	343.16	1192.7	343.15	1211.9	343.15	1230.1	343.15	1233.4	343.15	1239.0
348.17	1156.1	348.15	1178.4	348.15	1193.3	348.15	1215.6	348.15	1215.6	348.15	1225.1
353.15	1138.0	353.15	1162.4	353.15	1179.1	353.24	1200.1	353.15	1200.0		
SCS		SBT		SPF		SYG1		SYG2		PCS	
										298.15	1394.1
303.15	1369.2	303.15	1371.3	303.15	1371.3	303.38	1369.3	303.17	1365.2	303.23	1376.4
308.15	1353.3	308.17	1351.3	308.19	1351.4	308.17	1352.3	308.18	1345.4	308.21	1358.3
313.15	1335.9	313.15	1334.0	313.15	1332.1	313.28	1328.3	313.17	1326.4	313.15	1338.8
318.19	1314.4	318.15	1317.2	318.15	1314.4	318.17	1316.3	318.15	1309.8	318.15	1322.9
323.16	1298.2	323.45	1304.7	323.15	1297.3	323.22	1292.8	323.15	1292.8	323.15	1305.5
328.16	1283.4	328.17	1283.4	328.16	1278.2	328.16	1279.9	328.19	1275.5	328.18	1286.1
333.15	1264.8	333.17	1263.9	333.10	1263.1	333.17	1261.4	333.17	1258.0	333.15	1271.6
338.15	1250.1	338.16	1250.9	338.18	1247.6	338.18	1250.1	338.20	1242.6	338.20	1253.4
343.15	1230.1	343.15	1235.0	343.15	1231.0	343.16	1230.1	343.17	1225.3	343.15	1237.4
348.18	1216.4	348.15	1214.8	348.24	1215.7	348.16	1213.3	348.18	1211.7	348.18	1221.1
353.15	1203.1	353.15	1200.8	353.21	1200.8	353.17	1204.6	353.16	1194.7	353.17	1206.2

The uncertainty in u is less than ±1 $\mathrm{m\,s^{-1}}$.

Table 5
Fitting parameters of Eq. (4) fitted to the (u, T) data of this study.

Coefficient	MeC12:0	MeC14:0	MeC16:0	MeC18:0	MeC18:1	MeC18:2
u_0/ m·s^{-1}	2686.63 ± 149.84	3161.21 ± 229.98	2618.54 ± 397.50	3176.01 ± 519.87	2735.85 ± 156.48	2891.28 ± 107.69
u_1/ m·s^{-1} K^{-1}	−5.4044 ± 0.9220	−8.3242 ± 1.4152	−4.7717 ± 2.3882	−8.1501 ± 3.0764	−5.4332 ± 0.9625	−6.3177 ± 0.6784
u_2/ m·s^{-1} K^{-2}	$2.887 \times 10^{-3} \pm 1.4 \times 10^{-3}$	$7.550 \times 10^{-3} \pm 2.2 \times 10^{-3}$	$1.963 \times 10^{-3} \pm 3.6 \times 10^{-3}$	$7.235 \times 10^{-3} \pm 4.5 \times 10^{-3}$	$3.068 \times 10^{-3} \pm 1.5 \times 10^{-3}$	$4.387 \times 10^{-3} \pm 1.1 \times 10^{-3}$
N_p	12	12	9	7	12	13
R	1.000	1.000	1.000	1.000	1.000	1.000
σ/m·s^{-1}	1.3	2.0	1.55	1.05	1.33	1.18
AAD/%	0.08	0.1	0.09	0.06	0.06	0.07
Biodiesel	SCS	SBT	SPF	SYGI	SYG2	PCS
u_0/ m·s^{-1}	3132.04 ± 253.21	2591.71 ± 348.09	3542.03 ± 100.62	3732.82 ± 405.15	3201.08 ± 123.33	2989.51 ± 100.45
u_1/ m·s^{-1} K^{-1}	−7. 8994 ± 1.5457	−4.5707 ± 2.1251	−10.3988 ± 0.6142	−11.6045 ± 2.4727	−8.3564 ± 0.7529	−6.9645 ± 0.6181
u_2/ m·s^{-1} K^{-2}	$6.890 \times 10^{-3} \pm 2.4 \times 10^{-3}$	$1.784 \times 10^{-3} \pm 3.2 \times 10^{-3}$	$10.678 \times 10^{-3} \pm 9.0 \times 10^{-4}$	$12.573 \times 10^{-3} \pm 3.8 \times 10^{-3}$	$7.581 \times 10^{-3} \pm 1.1 \times 10^{-3}$	$5.418 \times 10^{-3} \pm 9.0 \times 10^{-4}$
N_p	11	11	11	11	11	12
R	1.000	0.999	1.000	0.999	1.000	1.000
σ/m·s^{-1}	1.7	2.4	0.7	2.7	0.9	0.9
AAD/%	0.105	0.127	0.036	0.162	0.380	0.05

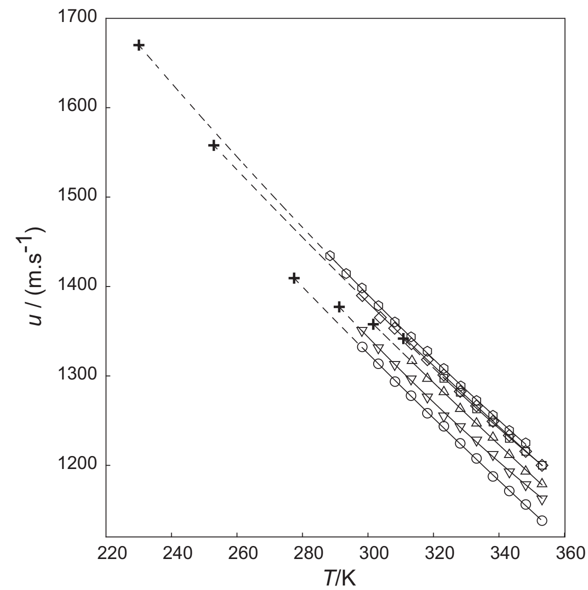

Fig. 3. Speed of sound of methyl esters (u) as function of the temperature (T) measured in this work. ○, MeC12:0; ▽, MeC14:0; △, MeC16:0; □, MeC18:0; ◇, MeC18:1; ⬡, MeC18:2; +, melting points [27].

and molar compressibility of the pure FAMEs. The results for molar compressibility are presented in Table 6 and depicted in Fig. 8a versus temperature. It is clearly observed that k_m is an almost constant function of temperature, tending to be lightly decreasing. Table 7 shows the coefficients k_1 and k_2 of the linear representation $k_m = -k_1 + k_2T$ as well as the standard deviations of the fitting. As the molar compressibility only is slightly temperature dependent, it seems logical to calculate the average values $\langle k_m \rangle = (1/N_p)\sum_i^{N_p}(k_m)_i$ for future applications. The $\langle k_m \rangle$ values of FAMEs are presented in Table 6 as well as the standard deviation from the mean value of molar compressibility, σ_{km}, and the average absolute deviation from the mean, AAD%. These quantities are, respectively, defined as

$$\sigma_{km} = \left[\sum_{i=1}^{N_p}(k_m - \langle k_m \rangle)_i^2/Np\right]^{1/2} \tag{8}$$

$$AAD\% = (100/N_p)\sum_{i=1}^{N_p}|1 - \langle k_m \rangle/k_m|_i \tag{9}$$

The standard deviation σ_{km} and the AAD% are usually lower than 5×10^{-3} and 0.05%, respectively. Also, one proceeded with the calculation of the molar compressibility for the biodiesel samples studied by Freitas et al. [12], Huber et al. [17], and the ones processed in this work. For the samples used by Freitas et al. and Huber et al. the density is known and was used. The calculated k_m values using Eq. (5), were obtained from the speed of sound and density of biodiesel fuels, presented by Freitas et al. [12] and Pratas et al. [30], respectively, and from the same data determined by Huber et al. [17]. For the processed synthetic samples and produced cotton seed biodiesel sample the density ρ was calculated by using the Kay mixing rule

$$\rho = \sum_i^{\text{FAMES}} x_i\rho_i \tag{10}$$

where ρ_i represents the density of FAME i in the mixture with molar fraction x_i. Pratas et al. [30] have shown that using molar fractions in Kay rule is preferable than the use of other concentration unit, and that the AAD% between calculated and experimental values of density were *ca.* 0.33%. The molar compressibility of biodiesel is

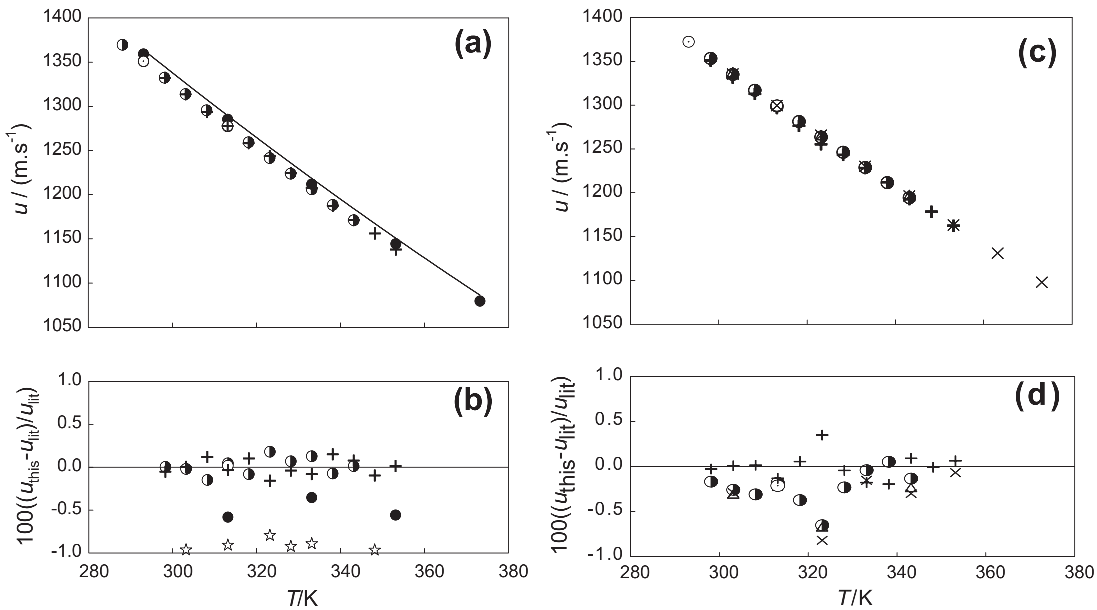

Fig. 4. Speed of sound (u) of MeC12:0 and MeC14:0 as function of the temperature (T) and comparison of experimental data of this work with the previous literature data. Legend: (a) values (u, T) for MeC12:0; (b) relative deviations for MeC12:0; (c) values (u, T) for MeC14:0; (d) relative deviations for MeC14:0. In the relative deviations (u_{this}) represent this works experimental data and (u_{lit}) the values from the literature. +, this work; ●, Tat and van Gerpen, NREL [11]; ⊙, Gouw and Vlugter [9]; ◑, Freitas et al. [12]; (—),Tat and van Gerpen [10]; ×, Daridon et al. [13]: △, Ndiaye et al. [14]. In (b, d) the symbol + represents the relative deviations between the fitted values with equation (4) and this works experimental data.

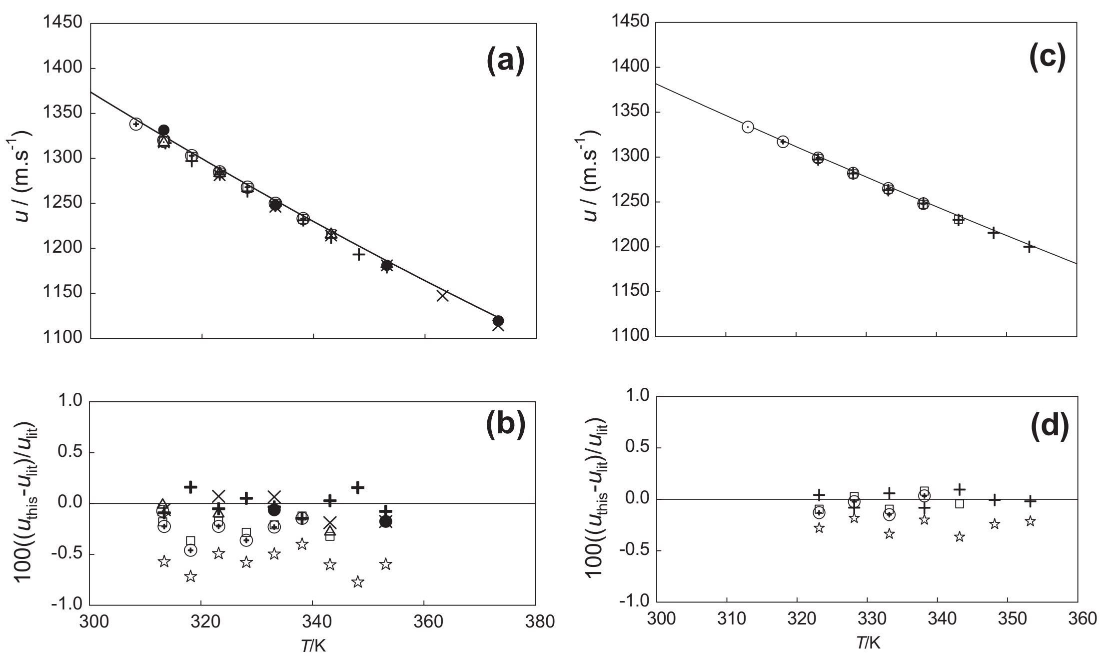

Fig. 5. Speed of sound (u) of MeC16:0 and MeC18:0 as function of the temperature (T) and comparison of experimental data of this work with the previous literature data. Legend: (a) values (u, T) for MeC16:0; (b) relative deviations for MeC16:0; (c) values (u, T) for MeC18:0; (d) relative deviations for MeC18:0. In the relative deviations (u_{this}) represent this works experimental data and (u_{lit}) the values from the literature. +, this work; ●, Tat and van Gerpen, NREL [11]; ⊙, Gouw and Vlugter [9]; (—),Tat and van Gerpen [10]; ☆, Tat and van Gerpen [10]; ×, Daridon et al. [13]; △, Ndiaye et al. [14]; ⊕, Ott et al. [15]; □, Freitas et al. [16]. In (b, d) the symbol + represents the relative deviations between the fitted values with equation (4) and this works experimental data.

presented in Table 6 and illustrated in Fig. 8b versus temperature. A statistical analysis of the biodiesel data was also performed calculating the standard deviation and the average absolute deviation from the mean value of the molar compressibility. The results are also shown in Table 6. The analysis of Fig. 8b allows us to conclude that for biodiesel, k_m is also slightly dependent of temperature, and this behavior is related to the nature of biodiesel sample (biodiesel composition). The standard deviation and the average absolute deviation from the mean value of k_m, are for all the biodiesel fuels, usually lower than 5×10^{-3} and 0.05%, respectively as verified for FAMEs.

Daridon et al. [13] observed a linear increase of the molar compressibility with the molecular weight for FAMEs and fatty acid ethyl esters (FAEE). This behavior is displayed in Fig. 9a, where the molar compressibility of saturated FAMEs (MeC8:0, MeC10:0, MeC12:0, MeC14:0, MeC16:0, MeC18:0) are represented as a

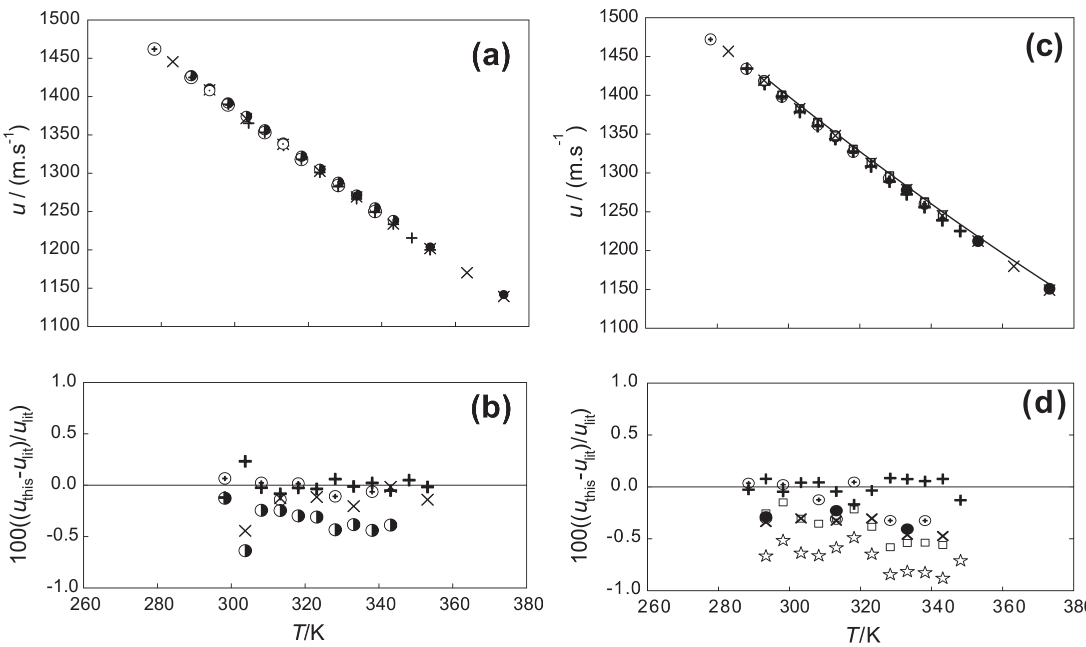

Fig. 6. Speed of sound (u) of MeC18:1 and MeC18:2 as function of the temperature (T) and comparison of experimental data of this work with the previous literature data. Legend: (a) values (u, T) for MeC18:1; (b) relative deviations for MeC18:1; (c) values (u, T) for MeC18:2; (d) relative deviations for MeC18:2. In the relative deviations (u_{this}) represent this works experimental data and (u_{lit}) the values from the literature. +, this work; ●, Tat and van Gerpen, NREL [11]; ⊙, Gouw and Vlugter [9]; ◑, Freitas et al. [12]; (—),Tat and van Gerpen [10]; ×, Daridon et al. [13]; ☆, Tat and van Gerpen [10]; ⊕, Ott et al. [15]; □, Freitas et al. [16]. In (b, d) the symbol + represents the relative deviations between the fitted values with equation (4) and this works experimental data.

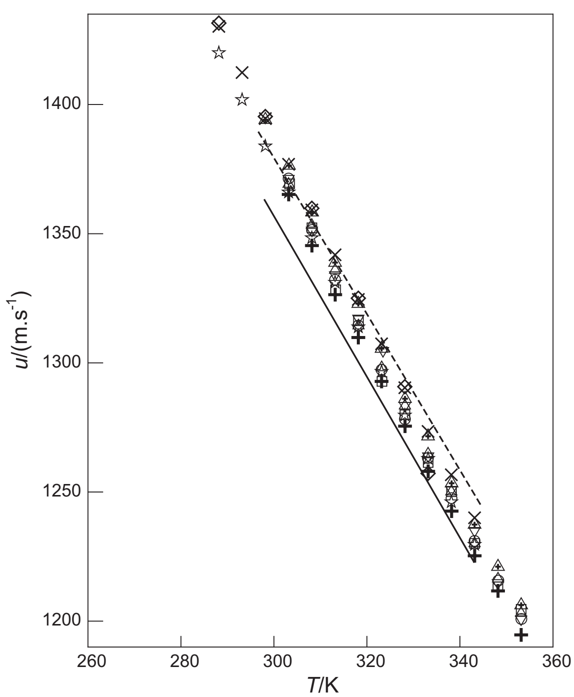

Fig. 7. Speed of sound of biodiesel (u) as function of temperature (T). Legend: △, SCS; ▽, SBT; ○, SPF; □, SYGI; +, SYGII; △, PCS; ×, Soy (S), Freitas et al. [12]; ☆, Palm (P), Freitas et al. [12]; (—), conventional diesel, Payri et al. [18]; (– –), Rapeseed biodiesel, Payri et al. [18]; ◇, Huber et al.[17].

function of molecular weight (M). The linear behavior can be described by the expression,

$$\langle k_m \rangle = -(0.2825 \pm 0.0049) + (0.02502 \pm 2.12 \times 10^{-5})M \quad (11)$$

which correlation coefficient, standard deviation, and AAD% are $R = 1.000$, $\sigma = \pm 0.0025$, and 0.03%, respectively. The unsaturated FAMEs MeC18:1, MeC18:2 and MC18:3 have lower values of molar compressibility than MeC18:0. Daridon et al. also observed similar straight lines for saturated FAMEs and FAEEs, which were coincidents, and also they were parallel to the corresponding line for paraffins. That means the molar compressibility is not only a function of molecular weight but depends on the molecular structure of molecules. The parallelism observed between paraffins and FAE is due to the constant contribution of the ester group for k_m in FAE, which is independent of the ester considered [13]. Based on these results, Daridon et al. developed a group contributionmethod for the prediction of k_m of FAE with AAD% less than 0.05%. It was checked the existence of some relationship between k_m and M for biodiesel with different compositions. In Fig. 9b the mean molar compressibility averaged to the temperature ranges of data, is represented as a function of the mean molecular weight of biodiesel, given by

$$M = \sum_{i}^{\text{FAMES}} x_i M_i \quad (12)$$

As before a linear behavior is also observed between $\langle k_m \rangle$ and M and considering the ($\langle k_m \rangle, M$) pairs for Freitas et al., Huber et al. and for our work (with the exception of SYG1 biodiesel because $\langle k_m \rangle$ is outside the observed range), the equation:

$$\langle k_m \rangle = (1.5630 \pm 0.2475) + (0.01839 \pm 0.0009)M \quad (13)$$

with correlation coefficient, standard deviation, and AAD% of, respectively, $R = 0.984$, $\sigma = \pm 0.0095$, and 0.11% was obtained. It is important to emphasize that this equation results from wide temperature and composition ranges of fuels. At extremes of molar weight are the values corresponding to the palm and soy biodiesel samples studied by Freitas et al. [12] presenting significant differences in composition: the palm sample (P) has composition (wt%)

Table 6
Molar compressibility (k_m) for FAME, synthetic and produced biodiesels.

T (K)	$k_m \times 10^3$	T (K)	$k_m \times 10^3$	T (K)	$k_m \times 10^3$	T (K)	$k_m \times 10^3$	T (K)	$k_m \times 10^3$	T (K)	$k_m \times 10^3$
MeC12:0		MeC14:0		MeC16:0		MeC18:0		MeC18:1		MeC18:2	
										288.41	6.967
										293.33	6.964
298.25	5.082	298.15	5.783					298.28	7.084	298.15	6.964
303.17	5.082	303.15	5.781					303.79	7.076	303.20	6.961
308.26	5.080	308.17	5.780					308.15	7.080	308.20	6.959
313.15	5.082	313.15	5.781	313.42	6.490			313.28	7.080	313.15	6.960
318.15	5.080	318.15	5.778	318.15	6.484			318.15	7.078	318.15	6.961
323.17	5.083	323.15	5.772	323.17	6.488	323.15	7.190	323.15	7.077	323.15	6.957
328.17	5.081	328.15	5.779	328.15	6.485	328.15	7.192	328.15	7.074	328.34	6.953
333.15	5.081	333.15	5.781	333.15	6.485	333.15	7.188	333.15	7.074	333.15	6.952
338.15	5.078	338.15	5.782	338.15	6.486	338.15	7.191	338.15	7.073	338.15	6.951
343.15	5.078	343.16	5.778	343.15	6.482	343.15	7.187	343.15	7.073	343.15	6.950
348.17	5.080	348.15	5.781	348.15	6.478	348.15	7.190	348.15	7.070	348.15	6.953
353.15	5.078	353.15	5.781	353.15	6.481	353.24	7.191	353.15	7.070		
$\langle k_m \rangle$	5.081	5.780		6.484		7.190		7.076		6.958	
σ_{km}	1.70×10^{-3}	2.72×10^{-3}		3.24×10^{-3}		1.47×10^{-3}		4.07×10^{-3}		5.36×10^{-3}	
AAD (%)	0.03	0.04		0.04		0.02		0.05		0.07	
SCS		SBT		SPF		SYG1		SYG2		PCS	
303.15	6.850	303.15	6.927	303.15	6.885	303.38	7.022	303.17	6.863	303.23	6.864
308.15	6.852	308.17	6.923	308.19	6.881	308.17	7.021	308.18	6.859	308.21	6.862
313.15	6.851	313.15	6.923	313.15	6.878	313.28	7.011	313.17	6.857	313.15	6.859
318.19	6.845	318.15	6.923	318.15	6.877	318.17	7.018	318.15	6.857	318.15	6.860
323.16	6.846	323.45	6.931	323.15	6.876	323.22	7.008	323.15	6.857	323.15	6.859
328.16	6.848	328.17	6.922	328.16	6.872	328.16	7.013	328.19	6.856	328.18	6.855
333.15	6.845	333.17	6.918	333.10	6.874	333.17	7.010	333.17	6.854	333.15	6.858
338.15	6.847	338.16	6.923	338.18	6.876	338.18	7.018	338.20	6.856	338.20	6.856
343.15	6.841	343.15	6.923	343.15	6.875	343.16	7.011	343.17	6.854	343.15	6.856
348.18	6.845	348.15	6.916	348.24	6.877	348.16	7.010	348.18	6.858	348.18	6.856
353.15	6.849	353.15	6.919	353.21	6.878	353.17	7.022	353.16	6.856	353.17	6.857
$\langle k_m \rangle$	6.847	6.923		6.877		7.015		6.857		6.859	
σ_{km}	3.09×10^{-3}	3.95×10^{-3}		3.28×10^{-3}		5.10×10^{-3}		2.48×10^{-3}		2.92×10^{-3}	
AAD (%)	0.04	0.04		0.04		0.07		0.03		0.04	

MeC16:0 = 42.45%, MeC18:1 = 41.92% and MeC18:2 = 9.80%, while for soy sample (S), MeC16:0 = 10.76%, MeC18:1 = 22.96% and MeC18:2 = 53.53%. From the data existent in the literature, it can be said that a narrow range is observed for the variation of molar weight (M_{min} = 284.317 corresponding to palm diesel to M_{max} = 295.072 for rapeseed fuel). Considering the molar compressibility and mean molar weight values of biodiesel samples prepared by Freitas et al., Huber et al. and the ones obtained in this work, resulted by least squares fitting the equation:

$$k_m = 6.8178 - 1.127 \times 10^{-4}T + F(M,T)(0.2351 - 6.8 \times 10^{-5}T) \tag{14}$$

with statistical parameters R = 1.000, σ = ±0.0102, and AAD% = 0.1%. In Eq. (14),

$$F(M,T) = -4.284 \times 10^{-7}(M - 295.07)(M - 284.32)T + 0.09298(M - 284.32) \tag{15}$$

This equation provides the accurate data of molar compressibility at molar weight limits M_{min} and M_{max}, before mentioned, therefore giving bounded values of k_m. The AAD% values from Eq. (14), related to the biodiesel fuels are given in Table 8. The error analysis is made considering the subsets (Freitas et al., Huber et al. and the ones obtained in this work), justified by the different variation range of sound speed versus temperature (see Fig. 7) and the different composition of fuels for the subsets. The results of Eq. (14) can be compared with those assuming the ideal mixing rule defined as:

$$k_m = \sum_{i}^{\mathrm{FAMES}} x_i k_{m,i} \tag{16}$$

where $k_{m,i}$ are the molar compressibility of the FAMEs. Due to the lack of experimental sound speed data for some minority FAMEs allowing the calculation of the molar compressibility, then in this work a pseudo-component concept similar to that applied by Freitas et al. [12] to the speed of sound was adopted: the molar compressibility of C16:1 was supposed as that of MeC16:0, that of MeC20:0, MeC22:0 and MeC24:0 as that of MeC18:0 and for MeC20:1 and MeC22:1 as that for C18:3. For methyl caprate (MeC10:0), the speed of sound provided by Daridon et al. [13] for temperatures ranging from 283.15 K to 343.15 K and density measured by Pratas et al. [31], were used to obtain the relation $k_m = 4.4151 - 1.0857 \times 10^{-4}\,T$. For methyl linolenate (MeC18:3) the speed of sound measured by Gouw and Vlugter [9] at temperatures of 293.15 K and 313.15 K and the density measured by Pratas et al. [32] provided a similar relation $k_m = 6.8400 - 3.9300 \times 10^{-5}T$.

From Table 8, it can be concluded that the predictions for the molar compressibility with the simple mixing rule given by Eq. (16), provide good estimates of that parameter. For Freitas et al. and this work subset, the AAD% is lower than 0.1%. The prediction with Eq. (14) is also possible with deviations lower than 0.1% particularly for Freitas et al. subset. The predictive capacity of both methods are evaluated in term of overall average deviation, OAAD%, defined as:

$$OAAD\% = \frac{1}{N_S}\sum_{i=1}^{N_S}(AAD\%)_i \tag{17}$$

where the subscript i refers to a subset with an average deviation value $(AAD\%)_i$ for the (T, k_m) data and N_s is the number of systems (subsets) involved. The OAAD% for equations (14) and (16) are 0.17 and 0.19%, respectively.

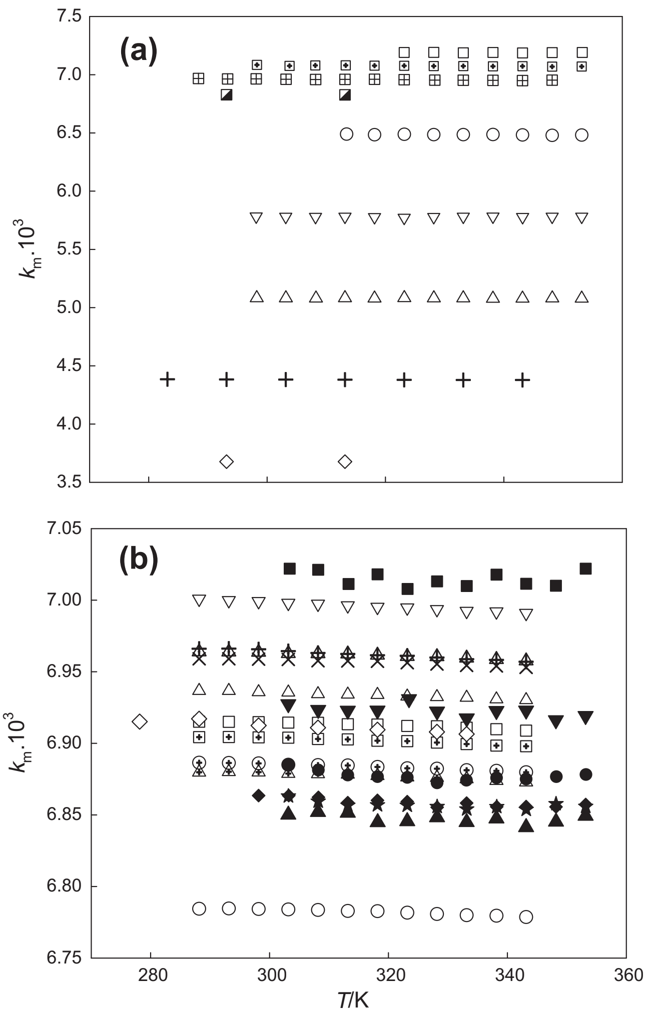

Fig. 8. Molar compressibility (k_m) of FAMES and biodiesel as a function of temperature (T). (a) FAMES: ◇, MeC8:0; +, MeC10:0; △, MeC12:0; ▽, MeC14 :0 ; ○, MeC16:0; □, methyl stearate; □, MeC18:0; ⊡, MeC18 :1; ⊞, MeC18:2; ◪, MeC18:3. (b) Biodiesel: △, soybean (S) [12]; ▽, rapeseed (R) [12] ; ○, palm (P) [12]; △, soybean+rapeseed (SR) [12];, palm+rapeseed (PR) [12]; △, soybean+palm (SP) [12]; □, soybean+rapeseed+palm (SRP) [12]; +, sunflower (SF) [12]; ×, (soybean+rapeseed) GP [12]; ⊡, SoyA [12] ; ◇, Sample A [17]; ▲, SCS; ▼, SBT; ●, SPF; ■, SYG1; ★, SYG2, ◆, PCS.

3.3. Models for speed of sound

From Eq. (6), the sound speed is obtained by

$$u = \rho^3 \left(\frac{k_m}{M}\right)^{7/2} \tag{18}$$

Therefore the sound speed can be calculated from the molar compressibility, density and molecular weight. As the molar compressibility can be considered as constant in wide ranges of temperatures $\langle k_m \rangle$ can be used in Eq. (18), giving

$$u = \rho^3 (\langle k_m \rangle / M)^{7/2} \tag{19}$$

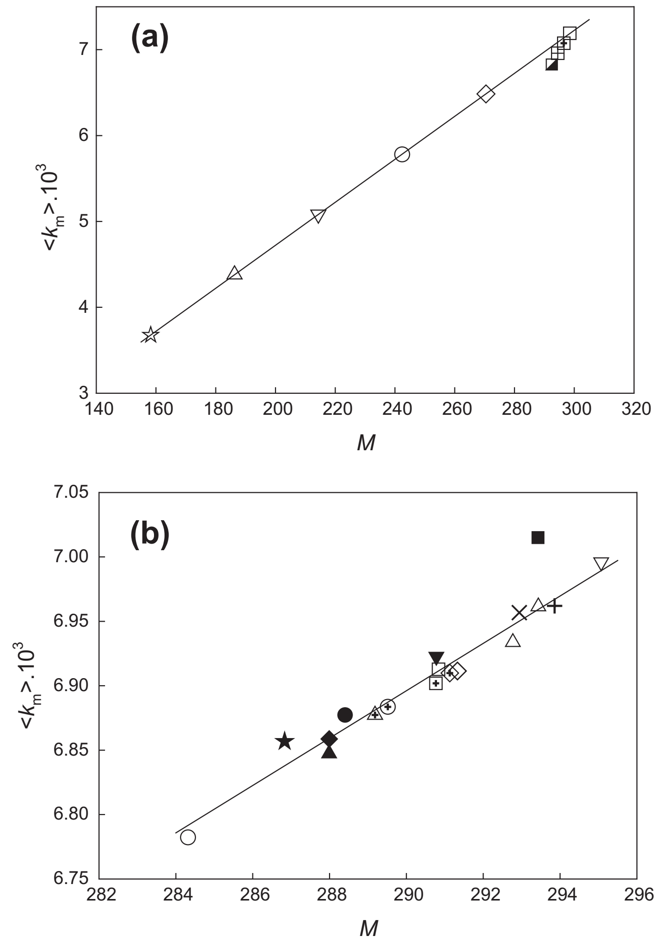

Fig. 9. Relation between molar compressibility (k_m) and molecular weight (M). (a) FAMES: ☆, MeC8:0; △, MeC10:0; ▽ MeC12:0; ○, MeC14:0; ◇, MeC:16; □, MeC18:0; ⊡, MeC18 :1; ⊞, MeC18:2; ◪, MeC18:3. (b) Biodiesel: △, S [12]; ▽, R [12] ; ○, P [12]; △, SR [12]; △, PR [12]; △, SP [12]; □, SRP [12]; +, Sf [12]; ×, GP [12]; ⊡, SoyA [12] ; ◇, Sample A and ◈, Sample B [17]; ▲,SCS; ▼, SBT; ●, SPF; ■, SYG1; ★, SYG2, ◆, PCS.

The density of FAMEs can be accurately calculated [31,32] or predicted while Kay mixing rule given by Eq. (10) can be used for biodiesel samples. Thus, Eq. (19) can be used to predict the speed of sound in FAMEs and biodiesel. The comparison between the sound speed calculated by Eq. (19) using Eq. (11) for $\langle k_m \rangle$, and experimental ones for saturated FAMES are given in Fig. 10. The individual AAD% values are expressed by Eq. (3), and are usually less than 0.20% (*ca.* 3 m s^{-1}), which is not far from the experimental error found in the measurements. For the saturated FAMEs the overall average relative deviation OAAD% was calculated by Eq. (17) where N_s refers to the number of FAMES studied. For the FAMEs (MeC6:0 to MeC18:0), the OAAD% = 0.15% (*ca.* 2 m s^{-1}). For FAMEs not included in the fit of Eq. (11) (MeCn:0, n = 7, 9, 11, 13, 15, 17) the OAAD% in the speed of sound is 0.26% (*ca.* 3 m s^{-1}).

Eq. (19) was applied to biodiesel fuels considering also the (T, u) subsets of Freitas et al. [12], Hubber et al. [17], and the six biodiesel

Table 7
Fitting parameters and standard deviation (σ) of linear of equation fitted to the (k_m, T) data.

Coefficients	MeC10:0	MeC12:0	MeC14:0	MeC16:0	MeC18:0	MeC18:1	MeC18:2	MeC18:3
k_1	4.4151 ± 0.0031	5.1007 ± 0.0081	5.7805 ± 0.0163	6.5523 ± 0.0187	7.1962 ± 0.0219	7.1455 ± 0.0104	7.0448 ± 0.0086	6.8400
k_2 10^5	−10.8571 ± 0.9939	−6.2091 ± 2.4734	−0.2170 ± 4.9955	−20.3650 ± 5-6001	−1.8152 ± 6.4877	−21.4394 ± 3.1809	−27.300 ± 2.7127	−3.9300
σ	0.001	0.002	0.003	0.002	0.002	0.002	0.002	0

Table 8
Error analysis of molar compressibility and speed of sound predictions by different methods.

Biodiesel	AAD% (k_m)			AAD% (u)						
	Eq. (14)	Eq. (16)	ID	VD	NMT	CT	MC1	MC2	JJ	IMP
S[a]	0.24	0.04	0.23	0.31	0.22	0.22	0.23	0.40	0.24	0.22
R[a]	0.00	0.02	0.27	0.34	0.27	0.26	1.86	0.99	0.28	0.26
P[a]	0.01	0.12	0.31	0.51	0.28	0.33	0.62	0.70	0.30	0.31
SR[a]	0.03	0.06	0.34	0.42	0.34	0.34	1.01	0.25	0.35	0.33
PR[a]	0.04	0.14	0.29	0.45	0.27	0.30	1.24	0.12	0.29	0.29
SP[a]	0.04	0.11	0.23	0.40	0.21	0.24	0.59	0.39	0.23	0.22
SRP[a]	0.01	0.11	0.31	0.46	0.29	0.31	1.02	0.08	0.31	0.30
SF[a]	0.14	0.02	0.32	0.37	0.31	0.31	0.69	0.07	0.32	0.31
GP[a]	0.04	0.13	0.23	0.31	0.22	0.22	0.82	0.08	0.24	0.22
SoyA[a]	0.14	0.18	0.33	0.42	0.32	0.34	0.54	0.36	0.34	0.33
PAAD%	0.07	0.09	0.28	0.40	0.27	0.29	0.86	0.34	0.26	0.22
HA[b]	0.18	0.31	0.40	0.45	0.39	0.40	0.74	0.08	0.41	0.39
HB[b]	0.14	0.52	0.37	0.43	0.37	0.37	1.12	0.32	0.38	0.37
PAAD%	0.16	0.42	0.39	0.44	0.38	0.39	0.93	0.06	0.40	0.38
SCS[c]	0.10	0.05	0.15	0.24	0.14	0.15	0.58	1.49	0.15	0.14
SBT[c]	0.19	0.04	0.14	0.20	0.14	0.14	0.63	0.34	0.14	0.14
SPF[c]	0.21	0.05	0.16	0.29	0.14	0.17	0.58	0.50	0.15	0.15
SYG1[c]	0.76	0.06	0.20	0.22	0.20	0.20	2.78	1.55	0.20	0.20
SYG2[c]	0.37	0.03	0.10	0.18	0.11	0.10	0.95	0.30	0.10	0.10
PCS[c]	0.06	0.15	0.52	0.64	0.49	0.54	0.14	0.96	0.52	0.51
PAAD%	0.28	0.06	0.21	0.30	0.20	0.21	0.94	0.86	0.21	0.21
OAAD%	0.17	0.19	0.29	0.38	0.28	0.30	0.91	0.42	0.29	0.27

[a] Freitas et al. [12].
[b] Hubbet et al. [17].
[c] Biodiesel fuels of this work. ID: ideal mixture; VD: van Dael; CT: Collision theory; MC1: Eq. (19) with density by Eq. (10); MC2: Eq. (19) with density of FAMEs by GCMOL method.

fuels of this work. The correlation (13) was used for the $\langle k_m \rangle$ calculation. The density of biodiesel was calculated in two ways because it is a fundamental property to be considered in Eq. (19). In a first method (MC1) the density was calculated by Eq. (10) using the density linear equations found by Pratas et al. [31,32] for the saturated and unsaturated FAMEs. In the second method, labeled as (MC2), the following relationship has been used,

$$\rho_{BD} = \left(\sum_i^{FAME} x_i M_i \Big/ \sum_i^{FAME} x_i V_{m,i} \right) \tag{20}$$

where the molar volume $V_{m,i}$ of the FAME i is calculated by GCVOL group contribution method revised by Pratas et al. [30].

Some predictive models usually used in the literature were also applied to calculate the speed of sound in biodiesel. As biodiesel is

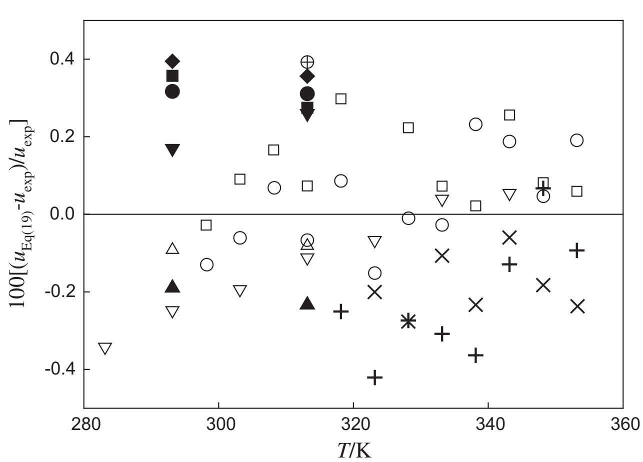

Fig. 10. Deviation between calculated speed of sound from Eq. (19) applied to FAMEs ($u_{EQ.}$ (19)) and experimental (u_{exp}). ▲, MeC7:0; △, MeC8:0; ▼, MeC9:0; ▽, MeC10:0; ●, MeC11:0; ○, MeC12:0; □, MeC13:0; ■, MeC14:0; ♦, MeC15:0; +, MeC16:0; ⊕, MeC17:0; ×, MeC18:0.

a mixture of FAMEs of similar molar weight one can use a mixing rule assuming an "ideal" mixture behavior, as

$$u_{BD} = \sum_i^{FAME} x_i u_i \tag{21}$$

In Eq. (21) the sound speed of FAME i was calculated for MeC12:0, MeC14:0, MeC16:0, MeC18:0, MeC18:1, and MeC18:2, using Eq. (4). For methyl caprate (MeC10:0) and methyl linolenate (MeC18:3) the (T,u) data of Daridon et al. [13] and Gouw and Vlugter [9] were considered, respectively. For MeC10:0, the data have given $u = 2802.4–6.2236T + 4.036 \times 10^{-3}T^2$ with standard deviation, $\sigma = 0.24\ \text{m s}^{-1}$ and for MeC18:3, it was found that $u = 2454.3–3.5050T$. The calculation of u_{BD} by Eq. (21) was made using again the pseudo-component concept similar to that applied to speed of sound by Freitas et al. [12] already explained. Other models are the equation of Van Dael [33] sometimes considered as a variation of ideal mixture, given as

$$u_{BD} = \left[\left(\sum_i^{FAME} \frac{x_i}{M_i u_i^2} \right) \left(\sum_i^{FAME} x_i M_i \right) \right]^{-1/2} \tag{22}$$

The Nomoto relation [34] written as

$$u_{BD} = \left(\sum_i^{FAME} x_i R_i \Big/ \sum_i^{FAME} x_i V_{m,i} \right) \tag{23}$$

where R_i and $V_{m,i}$ are the molar sound speed and the molar volume of FAME i, respectively. The molar sound speed is defined as $R = u^{1/3} V_m$[35]. Another model is the Schaaffs collision factor theory (CFT) [36–38]. Following this theory,

$$u_{BD} = u_\infty \left(\left(\sum_i^{FAME} x_i S_i \right) \left(\sum_i^{FAME} x_i B_i \right) / V_{mix} \right) \tag{24}$$

where $u_\infty = 1600\ \text{m s}^{-1}$, $S = (uV_m)/(u_\infty B)$ is the collision factor for the ith pure FAME in the biodiesel mixture. The molar volume of the mixture V_{mix} can be evaluated as $V_{mix} = (\sum_i^{FAME} x_i M_i / \rho_{mix})$ and

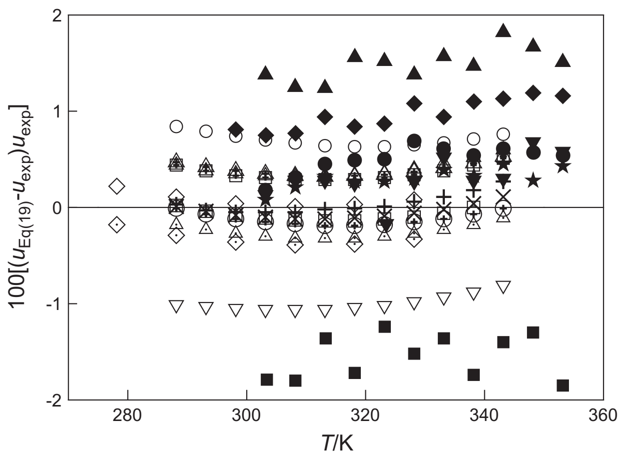

Fig. 11. Deviation between calculated speed of sound from Eq. (19) applied to biodiesel fuels (u_{EQ}(19)) and experimental (u_{exp}). △, S [12]; ▽, R [12]; ○, P [12];, SR [12]; ⊕, PR [12]; ⚠, SP [12]; □, SRP [12]; +, Sf [12]; ×, GP [12]; ⊞, SoyA [12]; ◇, Sample A and ◈, Sample B [17]; ▲, SCS; ▼, SBT; ●, SPF; ■, SYG1; ★, SYG2, ◆, PCS.

ρ_{mix} as evaluated using Eq. (10). B_i is the actual volume of a molecule per mole of FAME i in the biodiesel mixture which is evaluated as $B = 4/3\pi r^3 N_A$, where N_A is the Avogadro's number and r is the molecular radius of the pure FAME, calculated as $r = (3b/(16\pi N_A))^{1/3}$, where

$$b = \left(\frac{M}{\rho}\right) - \left(\frac{RT}{\rho u^2}\right)\left[\left(1 + \frac{Mu^2}{3RT}\right)^{1/2} - 1\right] \quad (25)$$

The Junjie relation [39],

$$u_{BD} = \left(\sum_i^{FAME} x_i V_{m,i}\right) \Big/ \left[\left(\sum_i^{FAME} (x_i M_i)^{1/2}\right)\left(\sum_i^{FAME} (x_i V_{m,i}/\rho_i u_i^2)\right)^{1/2}\right] \quad (26)$$

was also used to predict the speed of sound in biodiesel. Finally the speed of sound in biodiesel was also calculated based on the acoustical impedance ($Z = u\rho$),

$$u_{BD} = \left(\sum_i^{FAME} x_i Z_i \Big/ \sum_i^{FAME} x_i \rho_i\right) \quad (27)$$

The values of AAD% corresponding to the various methods described before are given in Table 8. The OAAD%, defined as in Eq. (17) with N_S identified with the number of biodiesel subsets ($N_S = 3$), is also presented in Table 8. The values of the partial AAD% (PAAD%), are presented for the different subsets of biodiesel fuels. The ideal mixture model which is the simplest to use, gives the same results compared with more sophisticated methods. It allows the representation of speed of sound data with OAAD = 0.29% being particularly good for our and Freitas et al. subsets. The ideal mixture method has equivalent predicting capacity as Nomoto, collision theory, Junjie, and impedance methods. The ideal mixture works better in our subset, being the individual values of AAD% of each biodiesel fuel lower compared with Freitas et al. and Hubber et al. subsets. This is perhaps due to the largest speed of sound variation range of our samples (see Fig. 7). The ideal mixture method was applied by Freitas et al. [12] to biodiesel fuels produced from different feedstocks. They obtained an OAAD% = 0.36%. In this work the value 0.28% was obtained and the difference is explained by the wide range of temperature tested by Freitas et al.. These same authors tried another prediction method based in a modified Auerbach model [12] but the results obtained were poor, being the deviations around 1.5%. It is interesting to see that Eq. (19) provides different AAD% values when different density calculation methods are used. The MC2 method which uses GCVOL group contribution gives usually lower deviations compared with MC1 one which uses Eq. (10). In our subset the deviations for PCS are higher than for the SCS although both fuels have the same composition (vd. Table 3). This is due to the higher speed of sound measured in PCS (vd. Table 4) and because it is possible that PCS contains other residual chemical species other than the detected FAMEs. The relative deviations between calculated and experimental speed of sound with the MC2 method is presented in Fig. 11. This method gives very good predictions of speed of sound particularly in Freitas et al. subset. More accurate relationships for $\langle k_m \rangle$ and k_m can be possibly developed and used with GCVOL method to give accurate estimates of speed of sound in biodiesel fuels.

4. Conclusions

The sound speed for six fatty acid methyl ester and six biodiesel fuels were measured at temperatures ranging from 288 to 353 K and at atmospheric pressure using a new non-intrusive method. For the six biodiesel samples five were prepared by weight from the pure FAMEs and one was produced from transesterification of cotton seed oil being characterized by gas chromatography. The speed of sound of FAMEs and biodiesel is very well described by polynomial quadratic equations in temperature. An extensive survey of speed of sound data in the literature was used for the purpose of comparison. The results produced in this work are in close agreement with the literature ones. A particular and interesting aspect is that the biodiesel samples of this work show a large variation range of speed of sound variation at a given temperature compared with the narrow range relative to the samples measured by Freitas et al. [12]. Taking the values of the density for FAMEs together with the sound speed data, the molar compressibilities were calculated. This property is a very weak function of temperature either for FAMEs or biodiesel and can be considered as a constant depending on the substance over wide temperature ranges. Deviations from mean value are usually less than 0.05%. Linear correlations were developed for mean molar compressibility as a function of molecular weight for FAMEs and biodiesel fuels with-AAD% of 0.03% and 0.11%, respectively. A new correlation for the molar compressibility of biodiesel as function of mean molecular weight and temperature was developed with mean overall deviation of 0.17% taking into account subsets of data from the literature and of this work. The deviation is less than 0.1% for several biodiesel fuels. For all the biodiesel the ideal mixture model which is the simplest to use has equivalent predictive capability of sound speed in biodiesel as the more sophisticated methods. The new method developed in this work, based in mean molar compressibility and in the GCVOL group contribution for density calculation of FAMEs, gives good estimates of speed of sound. More accurate relationships for $\langle k_m \rangle$ and k_m can be possibly developed and used with GCVOL method to give even more accurate estimates of speed of sound in biodiesel fuels. It is expected that the prediction methods here developed for molar compressibility and speed of sound could produce useful correlations for other biodiesel properties as the cetane number and other exhaust emission related issues.

Acknowledgments

This research is sponsored by FEDER funds through the program COMPETE – Programa Operacional Factores de Competitividade – and by national funds through FCT – Fundação para a Ciência e a Tecnologia, under the project PEst-C/EME/UI0285/2013, and was also supported by a grant, EADIC II – ERASMUS MUNDUS ACTION 2 LOT 13A UE Mobility Programme 2010-2401/001-001 – EMA2“.

The authors acknowledge the support from Eng. Maria João Bastos during the Gas Cromatography tests of biodiesel fuels undertaken in the Chemical Process Engineering and Forest Products Research Centre.

References

[1] Kumar S, Yadav JS, Sharma VK, Lim W, Cho JH, Kim J, et al. Physicochemical properties of jatropha curcas biodiesel + diesel fuel no. 2 binary mixture at T = (288.15–308.15) K and atmospheric pressure. J Chem Eng Data 2011;56:497–501.

[2] Benjumea P, Agudelo JR, Agudelo AF. Effect of the degree of unsaturation of biodiesel fuels on engine performance, combustion characteristics, and emissions. Energy Fuels 2011;25:77–85.

[3] Dermibas A, Dermibas I. Importance of rural bioenergy for developing countries. Energy Conv Manage 2007;48:2386–98.

[4] Ruwwe J. Metal alkoxides as catalysts for the biodiesel production. Chem Today 2008;26(1):26–8.

[5] Martyn J, Earle MJ, Plechkova NV, Seddon KR. Green synthesis of biodiesel using ionic liquids. Pure Appl Chem 2009;81:2045–57.

[6] Bournay L, Casanave D, Delfort B, Hillion G, Chodorge JA. New heterogeneous process for biodiesel production: a way to improve the quality and the value of the crude glycerin produced by biodiesel plants. Catal Today 2005;106:190–2.

[7] Pogorevc P, Kegl B, Skerget L. Diesel and biodiesel fuel spray simulations. Energy Fuels 2008;22:1266–74.

[8] Tat ME, Gerpen J. Measurement of biodiesel speed of sound and its impact on injection timing. National renewable energy laboratory 2003; NREL/SR-510-31462.

[9] Gouw TH, Vlugter JC. Physical properties of fatty acid IV ultrasonic sound velocity methyl esters. J Am Oil Chem Soc 1964;41:524–6.

[10] Tat M, Gerpen J. Speed of sound and isentropic bulk modulus of alkyl monoesters at elevated temperatures and pressures. J Am Oil Chem Soc 2003;80:1249–56.

[11] Tat M, Gerpen J. Measurement of biodiesel speed of sound and its impact on injection timing. National renewable energy laboratory 2003; NREL/SR-510-31462.

[12] Freitas SVD, Paredes MLL, Daridon J, Lima AS, Coutinho JAP. Measurement and prediction of the speed of sound of biodiesel fuels. Fuel 2013;103:1018–22.

[13] Daridon J, Coutinho JAP, Ndiaye H, Paredes M. Novel data and a group contribution method for the prediction of the speed of sound and isentropic compressibility of puré fatty acid methyl and ethyl esters. Fuel 2013;105:465–70.

[14] Ndiaye HI, Habrioux M, Coutinho JAP, Paredes MLL, Daridon JL. Speed of sound, density, and derivative properties of ethyl myristate, methyl myristate, and methyl palmitate under high pressure. J Chem Eng Data 2013;58:1371–7.

[15] Ott L, Huber M, Bruno T. Density and speed of sound measurements on five fatty acid methyl esters at 83 kPa and temperatures from (278.15 to 338.15) K. J Chem Eng Data 2008;53:2412–6.

[16] Freitas SVD, Cunha DL, Reis RA, Lima AS, Daridon JL, Coutinho JAP, et al. Application of Wada's group contribution method to the prediction of the speed of sound of biodiesel. Energy Fuels 2013;27:1365–70.

[17] Huber ML, Lemmon EW, Kazakov A, Ott LS, Bruno TJ. Model for the thermodynamic properties of a biodiesel fuel. Energy Fuels 2009;23:3790–7.

[18] Payri R, Salvador FJ, Gimeno J, Bracho G. The effect of temperature and pressure on thermodynamic properties of diesel and biodiesel fuels. Fuel 2011;90:1172–80.

[19] Nikolić BD, Kegl B, Marcović SD, Mitrović MS. Determining the speed of sound, density and bulk modulus of rapeseed oil, biodiesel and diesel fuel. Therm Sci 2012;16(Suppl. 2):S569–79.

[20] Wadumesthrige K, Smith J, Wilson J, et al. Investigation of the parameters affecting the cetane number of biodiesel. J Am Oil Chem Soc 2008;85:1073–81.

[21] Ramírez-Verduzco L, Rodríguez-Rodríguez J, Jaramillo-Jacob A. Predicting cetane number, kinematic viscosity, density and higher heating value of biodiesel from its fatty acid methyl ester composition. Fuel 2012;91(1):102–11.

[22] Kinast J. Production of biodiesel from multiple feedstocks and properties of biodiesels and biodiesel/diesel blends. National renewable energy laboratory 2003; NREL/SR-510-31460.

[23] Canacki M, Gerpen JH. Comparison of engine performance and emissions for petroleum diesel fuel, yellow grease biodiesel, and soybean oil biodiesel. Trans ASAE 2003;46:937–44.

[24] http://webbook.nist.gov/chemistry/fluid/ (assessed May 2013).

[25] Fortin T, Laesecke A, Freund M. Advanced calibration, adjustment and operation of a density and sound speed analyzer. J Chem Thermodyn 2013;53:276–85.

[26] Zorębski E, Dzida M. The effect of temperature and pressure on acoustic and thermodynamic properties of 1,4-butanediol. The comparison with 1,2-, and 1,3-butanediols. J Chem Thermodyn 2012;54:100–7.

[27] Knothe G, Dunn RO. A comprehensive evaluation of the melting points of fatty acid sand esters determined by differential scanning calorimetry. J Am Oil Chem Soc 2009;86:843–6.

[28] Wada Y. On the relation between compressibility and molal volume of organic liquids. J Phys Soc Jpn 1949;4:280–3.

[29] Mathur SS, Gupta PN, Sinhat SC. Theoretical derivation of Wadás and Raós relations. J Phys A: Gen Phys 1971;4:434–6.

[30] Pratas MJ, Freitas SVD, Oliveira MB, Monteiro SC, Lima AS, Coutinho JAP. Biodiesel density: experimental measurements and prediction models. Energy Fuels 2011;25:2333–40.

[31] Pratas MJ, Freitas S, Oliveira MB, Monteiro SC, Lima AS, Coutinho JAP. Densities and viscosities of fatty acid methyl and ethyl esters. J Chem Eng Data 2010;55:3983–90.

[32] Pratas MJ, Freitas S, Oliveira MB, Monteiro SC, Lima AS, Coutinho JAP. Densities and viscosities of minority fatty acid methyl and ethyl esters present in biodiesel. J Chem Eng Data 2011;56:2175–80.

[33] Van Dael W, Vangael E. In: 1st International conference on calorimetry and thermodynamics, Warsaw, Poland; 1969, p. 555.

[34] Nomoto O. Empirical formula for sound velocity in liquid mixtures. J Phys Soc Jpn 1958;13:1528–32.

[35] Rao MM. The adiabatic compression of liquids. J Chem Phys 1946;14:699.

[36] Schaafs W. Molekularakustik. Berlin: Springer-Verlag; 1963.

[37] Jacobson B. Ultrasonic velocity in liquids and liquid mixtures. J Chem Phys 1952;20:927–8.

[38] Nutsch-Kuhnkies R. Sound velocities of binary mixtures and solutions. Acoustica 1965;15:383–6.

[39] Junjie Z. J. China Univ Sci Tech 1984;14:298–300.